Electronic Supplementary Material (ESI) for Biomaterials Science.

Supporting Information:

Liposomal MRI probes containing encapsulated or amphiphilic Fe(III) coordination complexes

*Md Saiful I. Chowdhury,[1] Elizabeth A. Kras,[1] Steven G. Turowski,[2] Joseph A. Spernyak[2] and Janet R. Morrow[1]**

[1] Department of Chemistry, University at Buffalo, The State University of New York

Amherst, NY 14260, United States

[2] Department of Cell Stress Biology, Roswell Park Comprehensive Cancer Center, Buffalo, New York 14263, United States

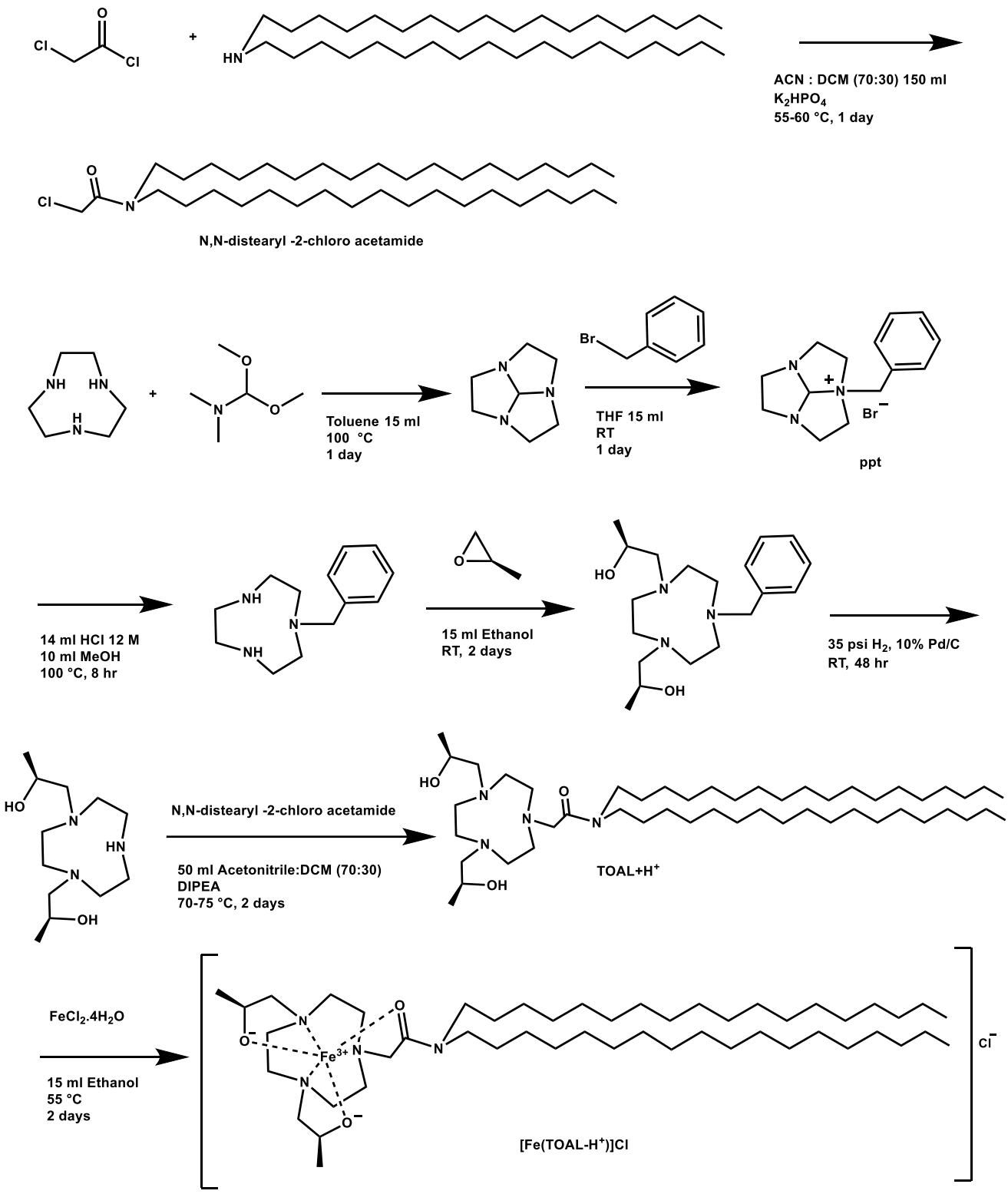

Scheme S1. Synthesis of N,N-distaeryl-2-chloro acetamide, TOAL+ H^+ ligand and Fe(III) complex

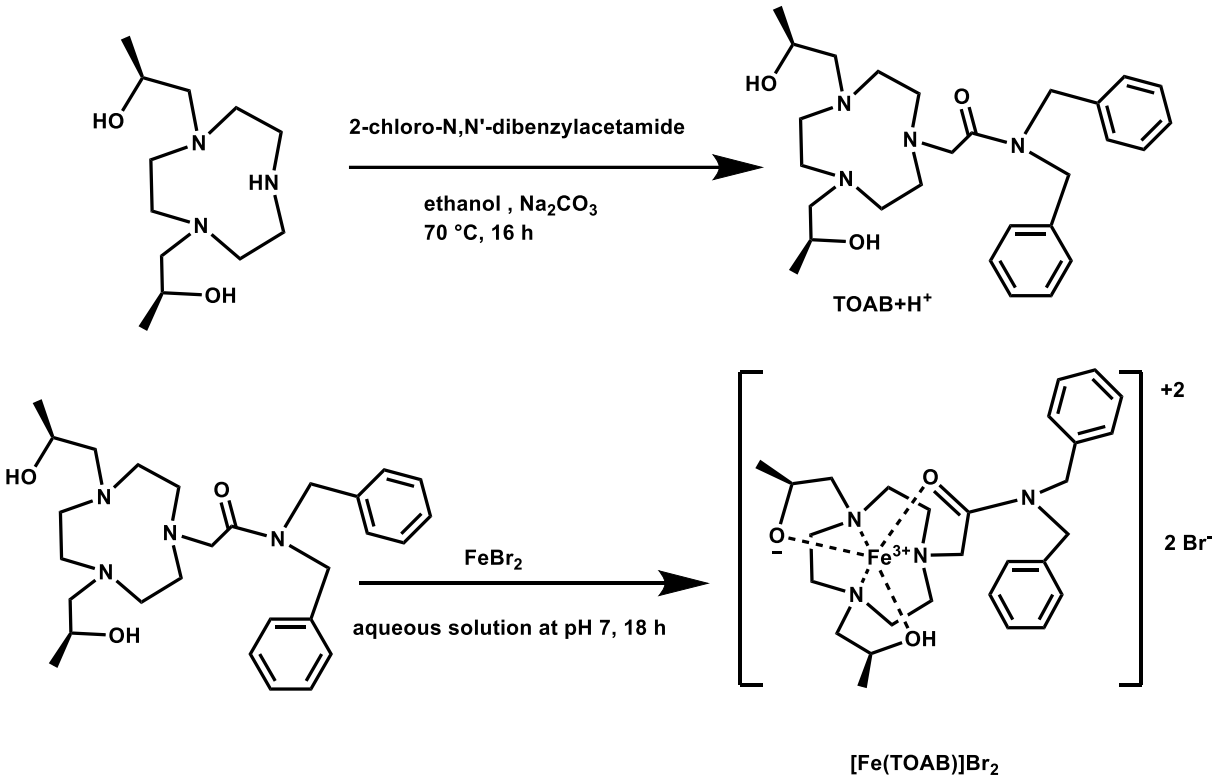

Scheme S2. Preparation of TOAB+H^+ ligand and Fe(III) complex

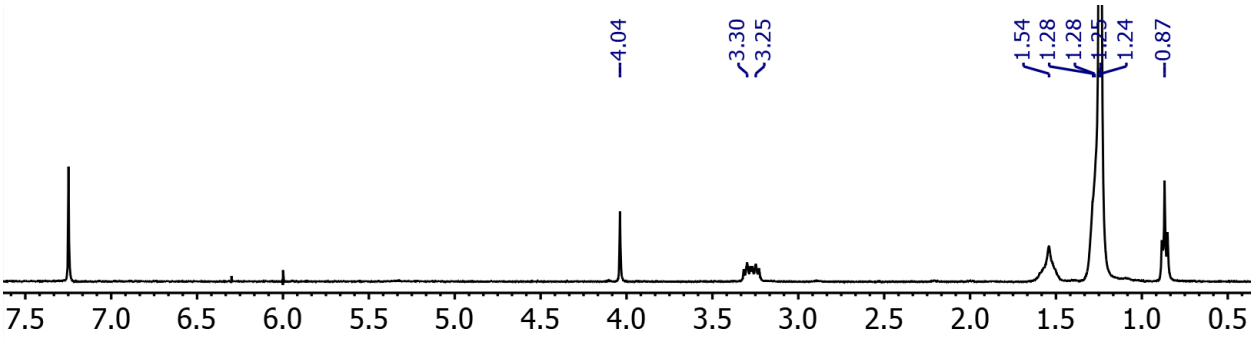

Figure S1a. ^{1}H NMR of N,N-distaeryl-2-chloro acetamide in $CDCl_3$

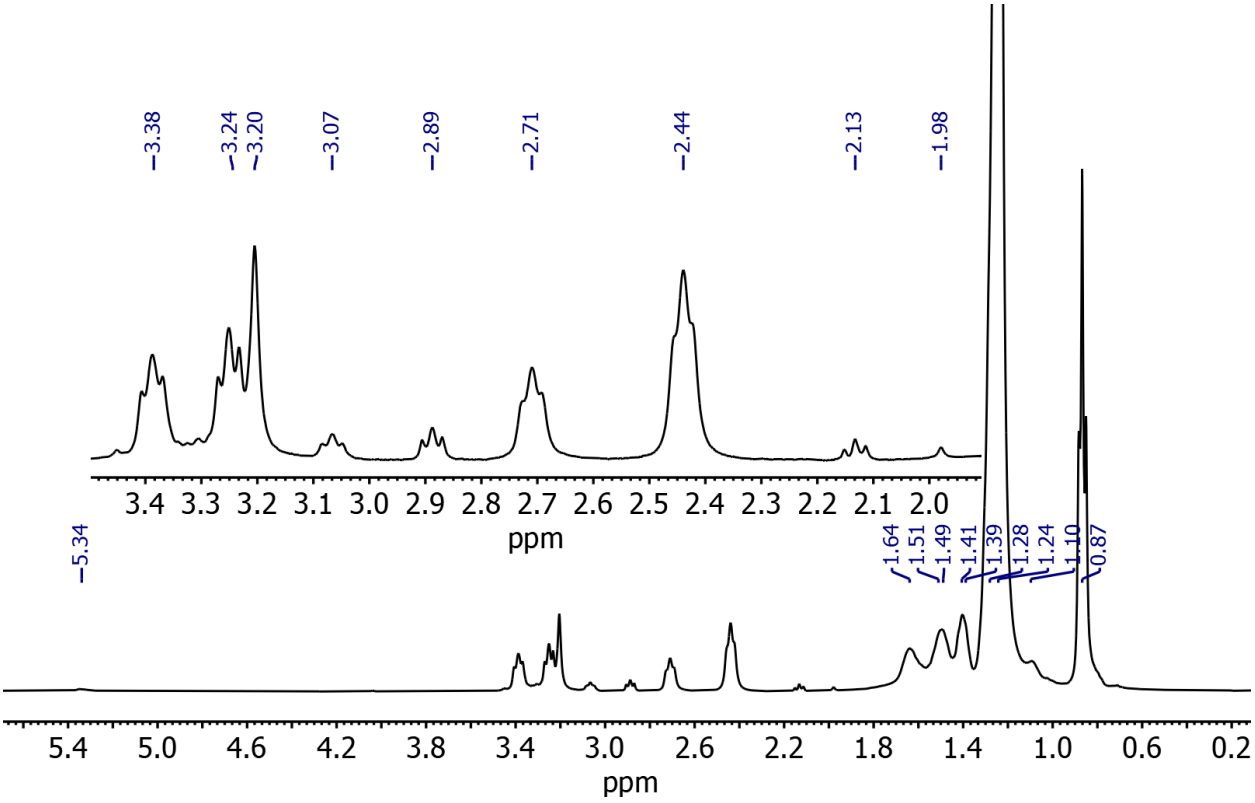

Figure S1b. ^{1}H NMR of TOALH ligand in $CDCl_3$

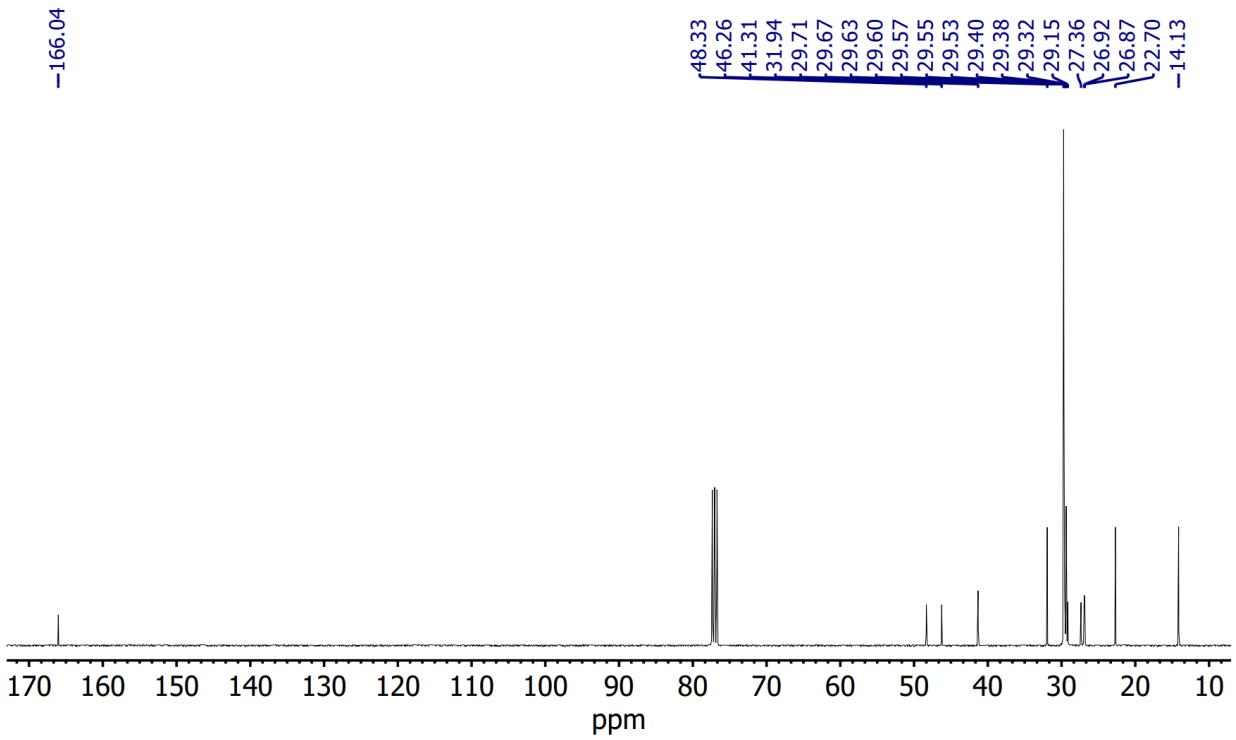

Figure S2a. ^{13}C NMR of N,N-distaeryl-2-chloro acetamide in $CDCl_3$

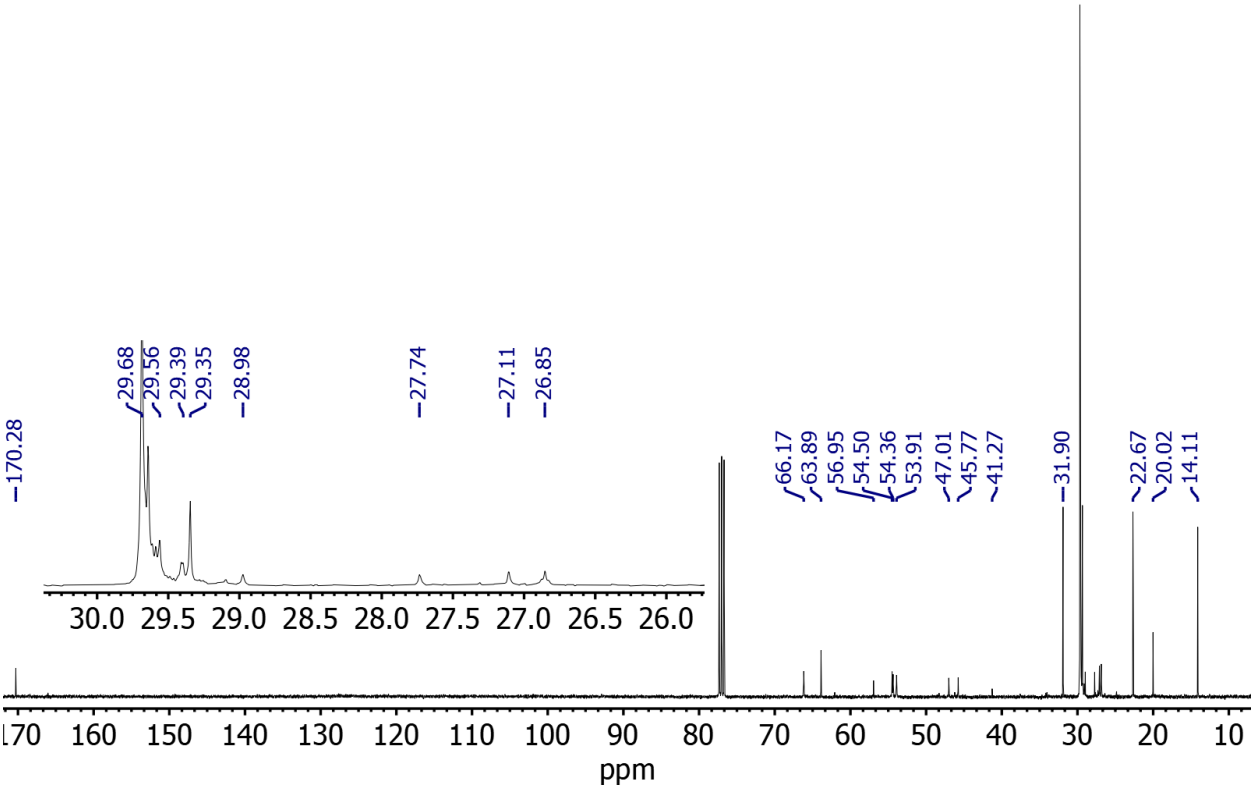

Figure S2b. ^{13}C NMR of TOALH ligand in $CDCl_3$

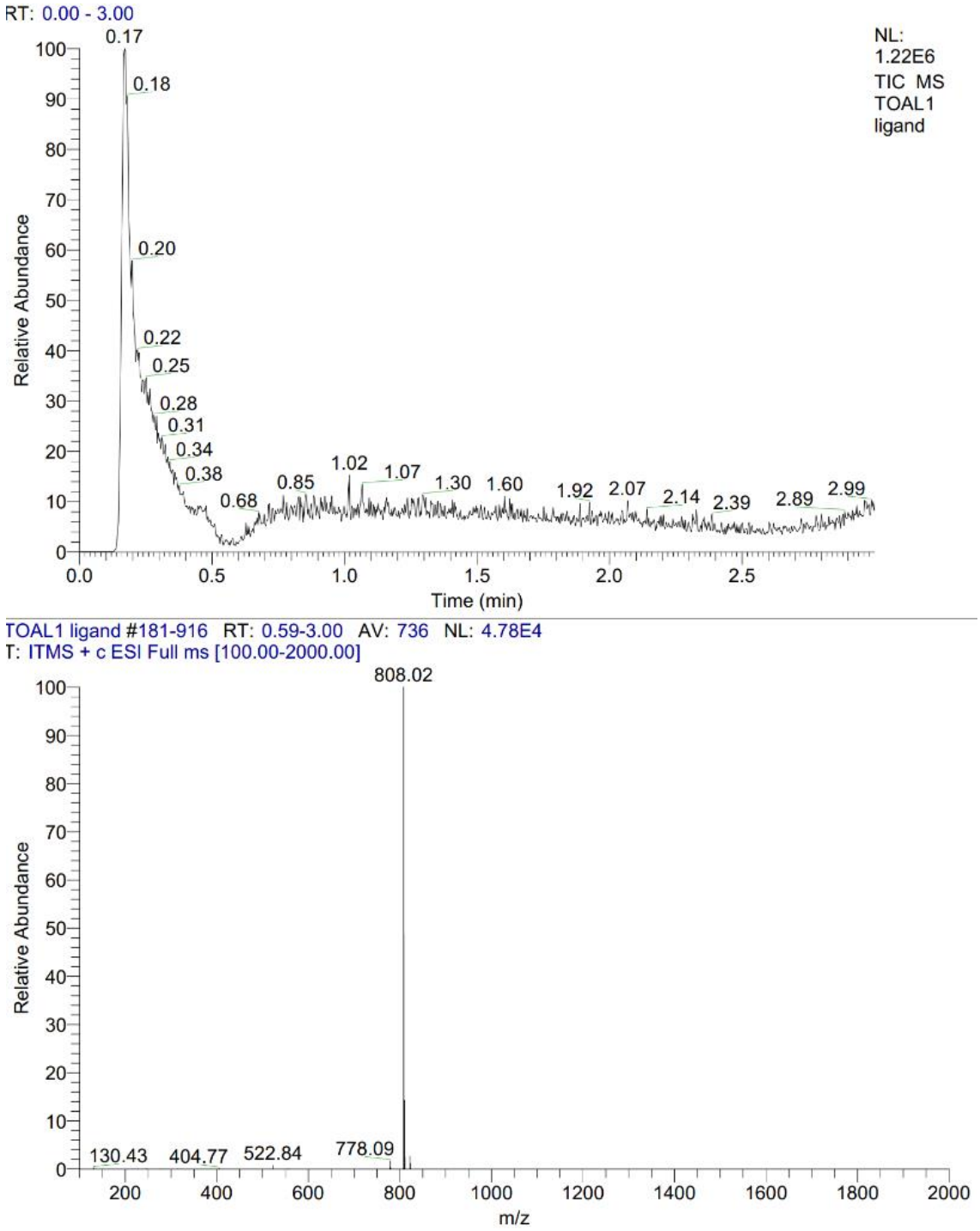

Figure S3. ESI-MS of TOALH ligand

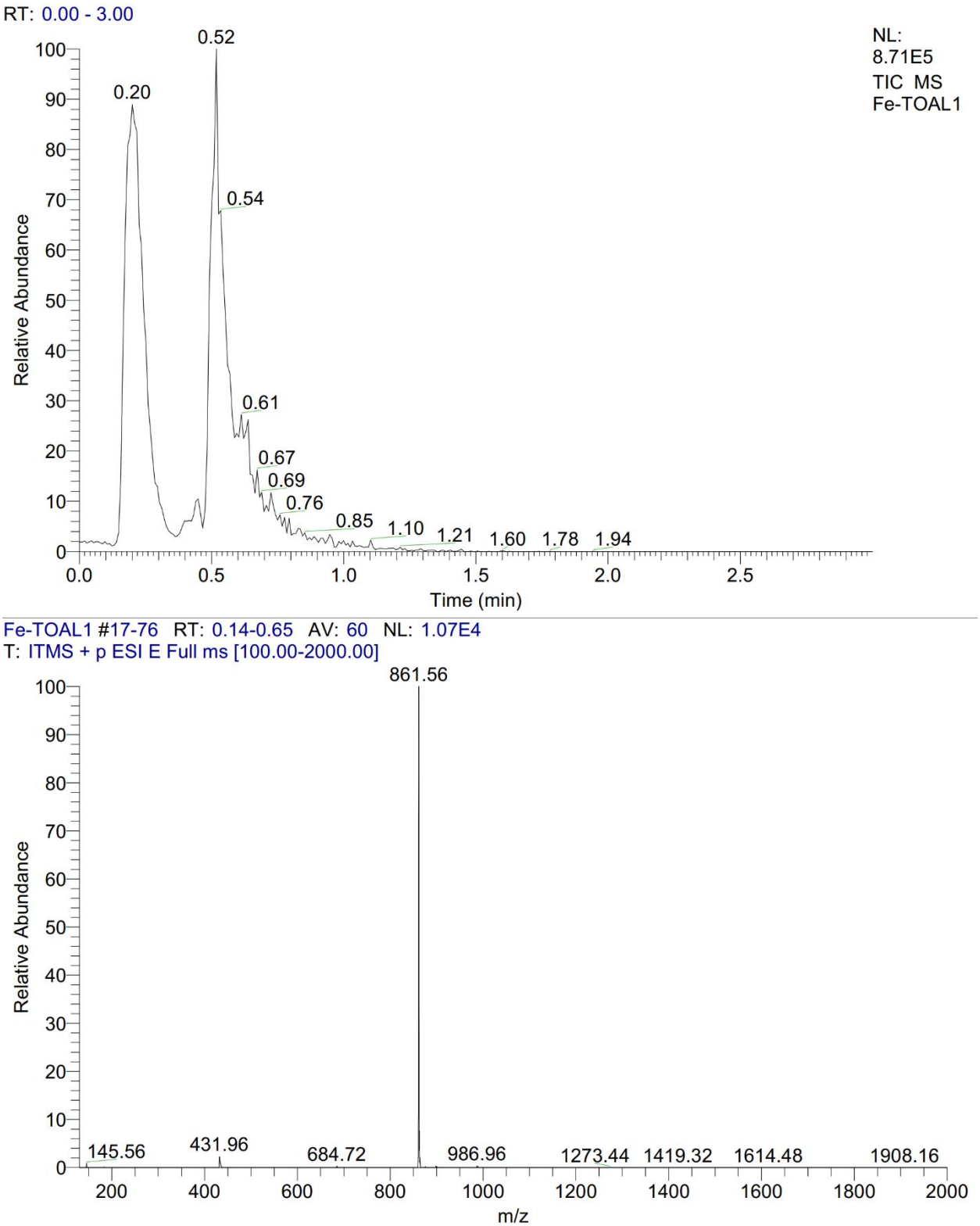

Figure S4. ESI-MS of [Fe(TOAL-H$^+$)]Cl. M$^+$ = [Fe(TOAL-H$^+$)]$^+$

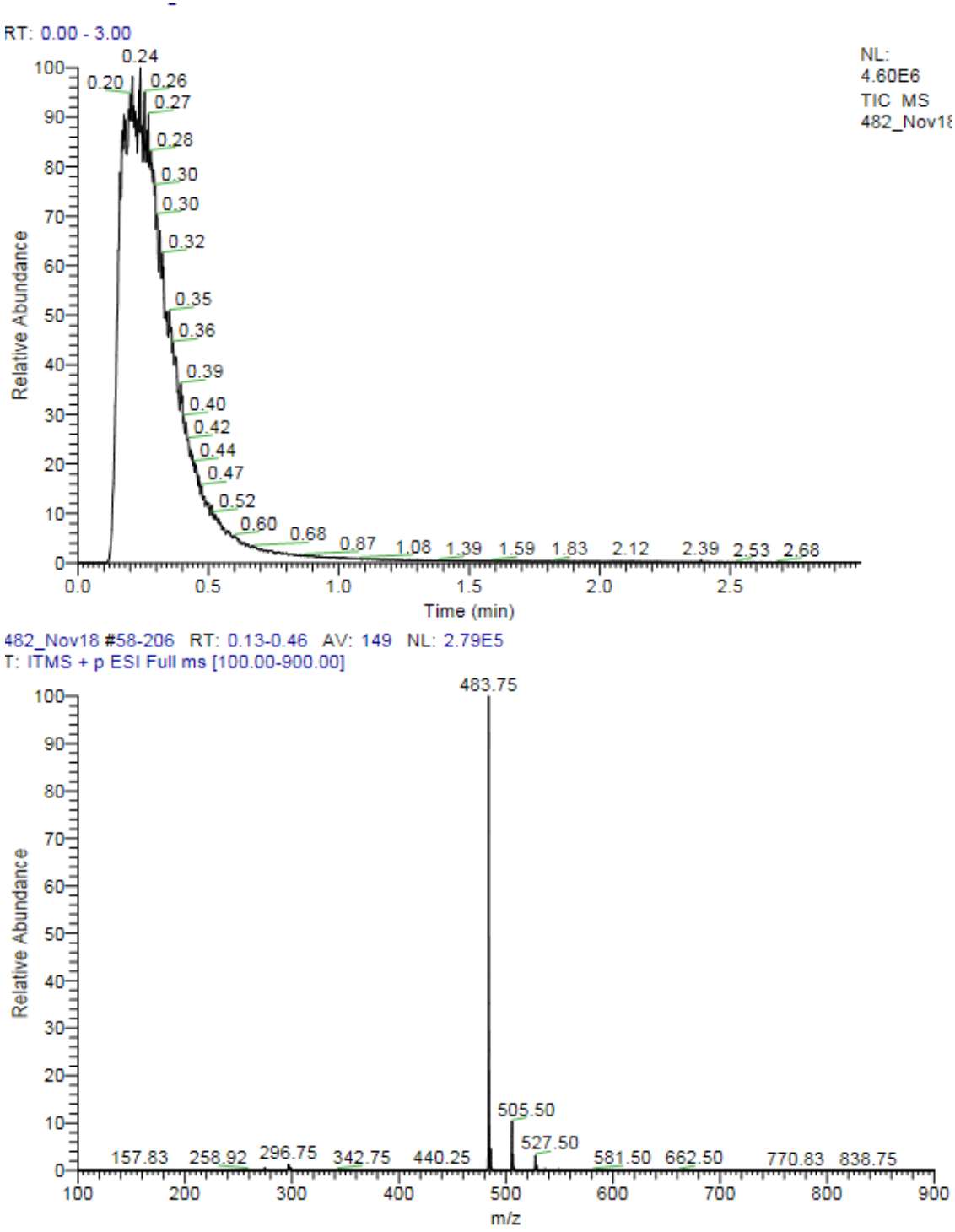

Figure S5. ESI-MS of TOABH (483.75). TOAB+Na^+ (505.50)

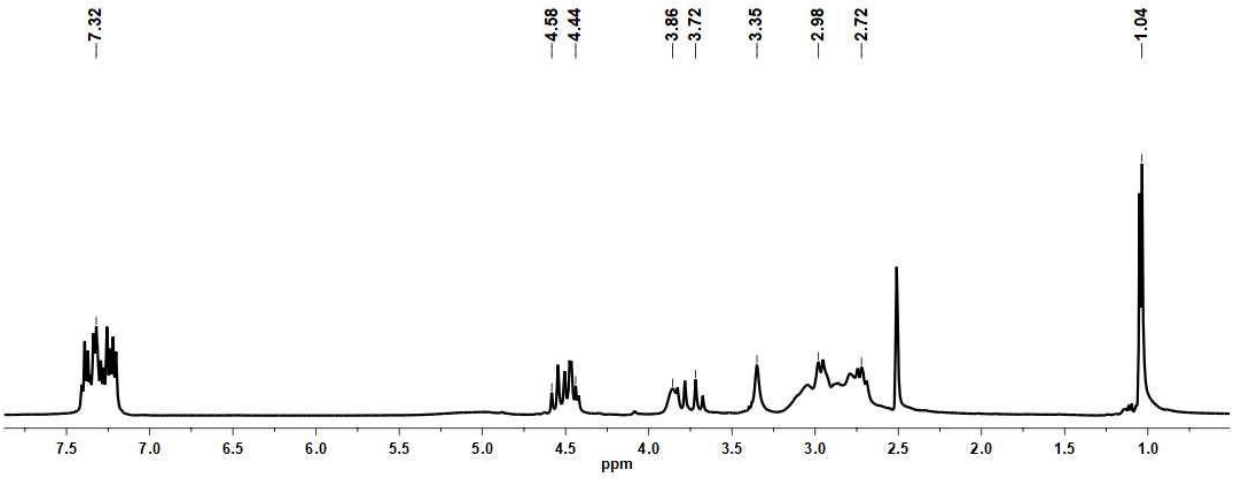

Figure S6. ^{1}H NMR of TOABH ligand in DMSO-D_6.

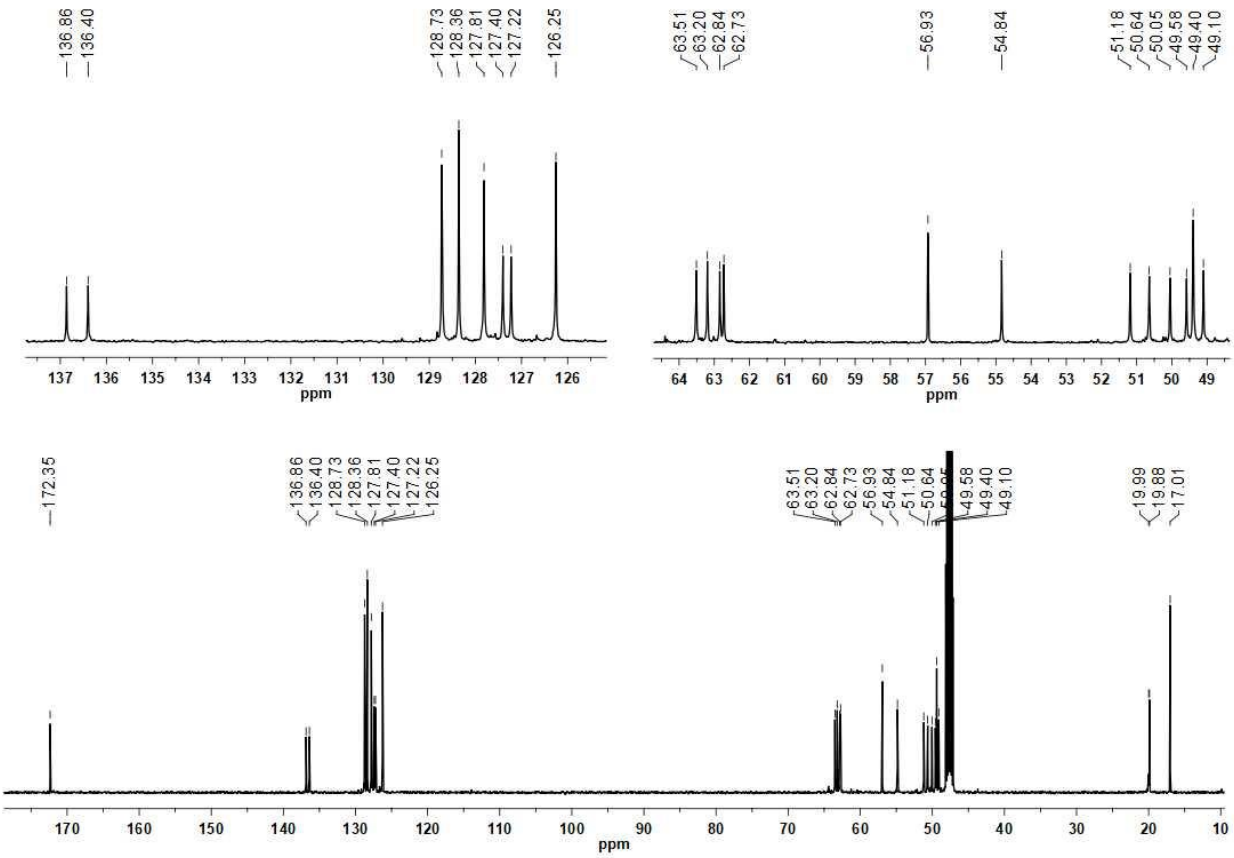

Figure S7. ^{13}C NMR of TOABH ligand in MeOD

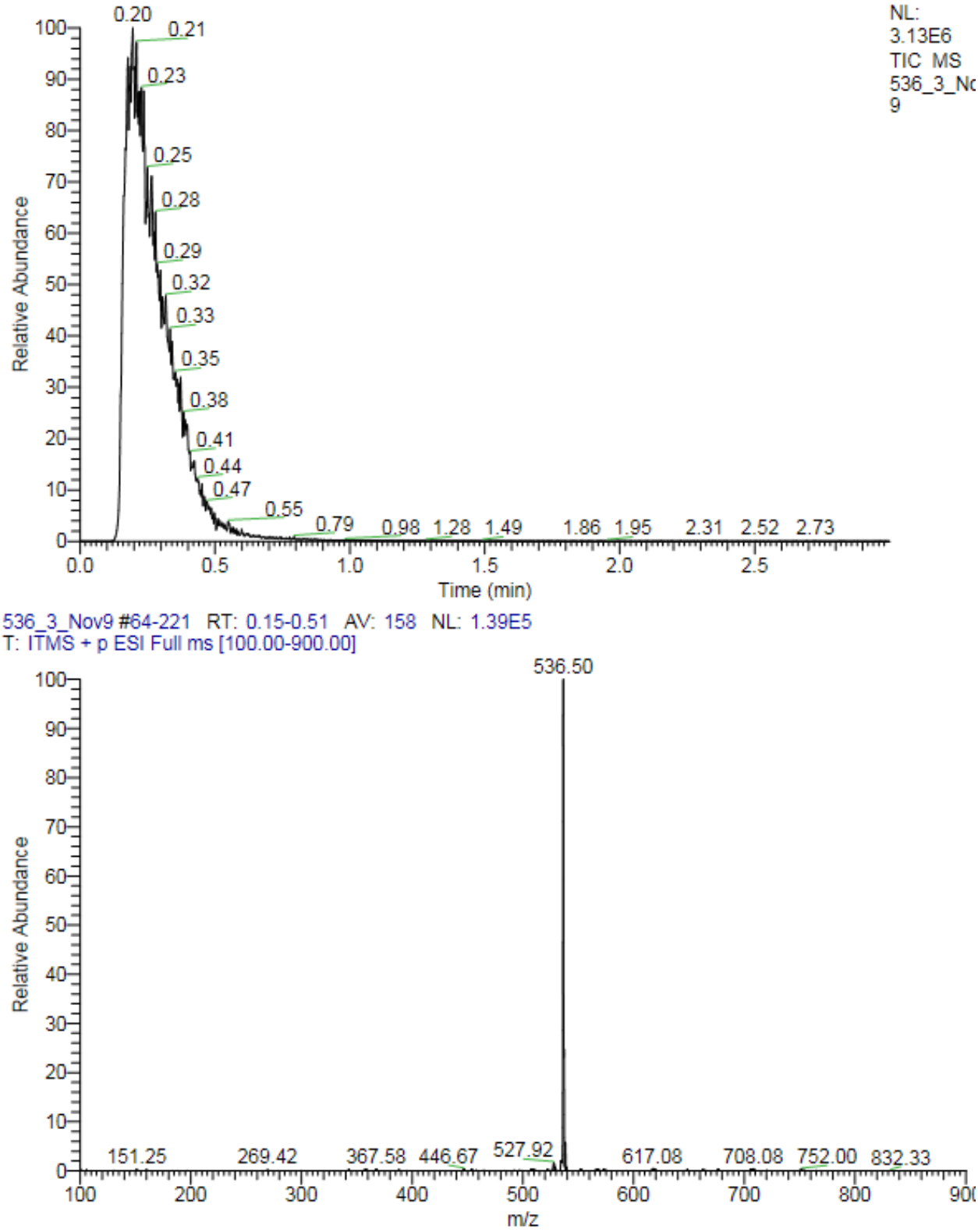

Figure S8. ESI-MS of $[Fe(TOAB)]Br_2$. $M^+ = [Fe(TOAB\text{-}H^+)]^+$

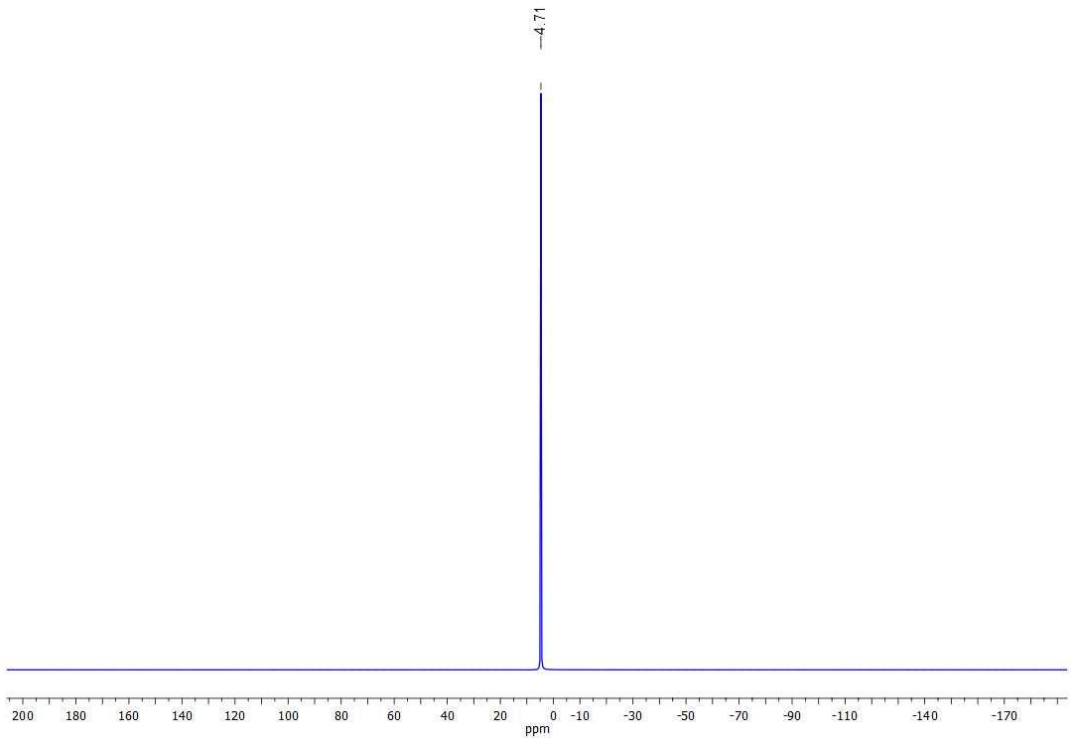

Figure S9. ^{1}H Spectrum of [Fe(TOAB)]Br_2 at 15.0 mM (500 MHz, D_2O, 298K)

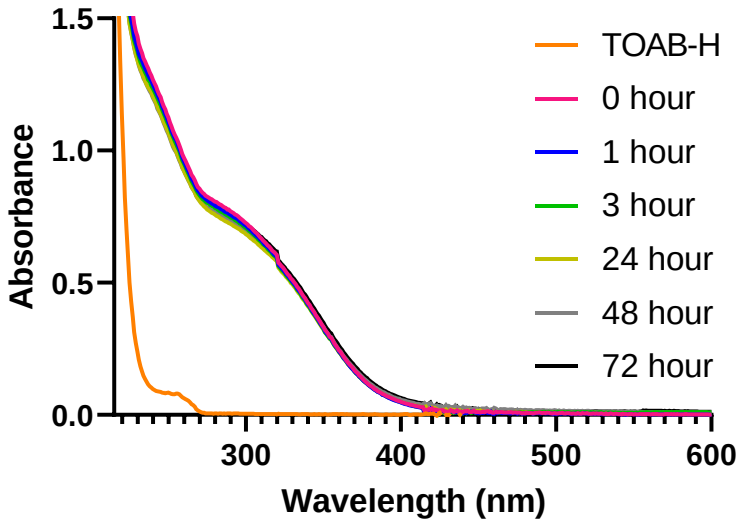

Figure S10. UV-Vis absorbance spectra of TOAB-H ligand and [Fe(TOAB)]Br_2; TOAB-H solution contained 0.20 mM ligand. Fe solution contained 0.20 mM [Fe(TOAB)]Br_2 in 1x PBS Buffer (pH 7.1) and was incubated a 37 °C for 72 hours

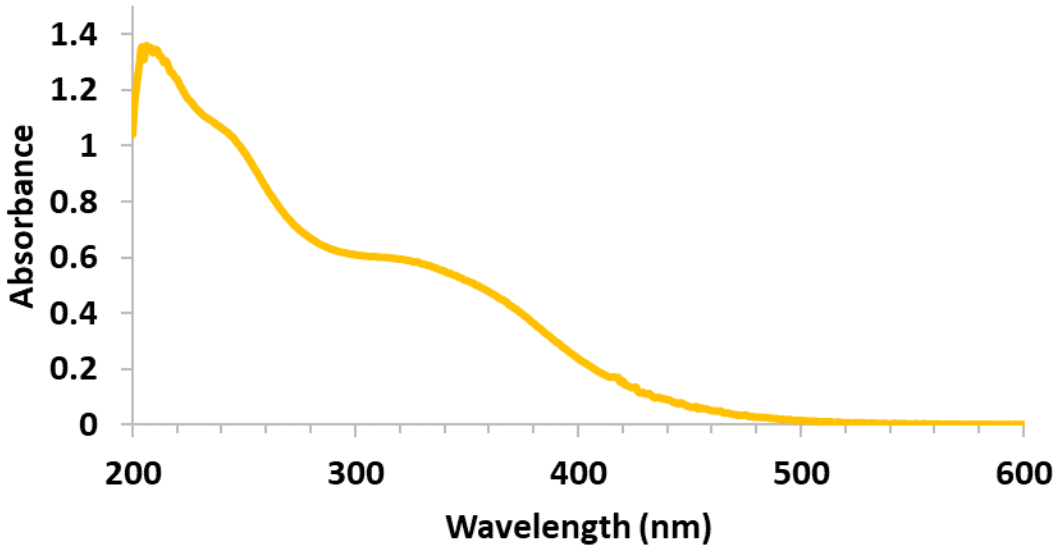

Figure S11. UV-Vis absorbance spectra of 145 µM [Fe(TOAL-H^+)]Cl in methanol at 37 °C

Complex	Wavelength (nm)	Molar absorptivity ($M^{-1}cm^{-1}$)
[Fe(TOAB)]Br_2	300	3.83×10^3
[Fe(TOAL-H^+)]Cl	206	9.40×10^3
	247	6.98×10^3
	332	3.97×10^3

Table S1. Molar absorptivity ($M^{-1}cm^{-1}$) of the complexes at 37 °C

	Time	R_1 (s^{-1}) saline	R_2(s^{-1}) saline	R_1(s^{-1}) serum	R_2(s^{-1}) serum
LipoA	1 day	0.67	4.9	0.65	2.6
	2 day	0.69	5.0	0.76	2.8
LipoC	1 day	0.93	5.5	2.3	8.5
	2 day	0.88	5.5	2.8	8.0
LipoB	1 day	2.8	20	2.1	9.7
	2 day	2.8	19	2.0	12

Table S2. Relaxivity of liposomes over time measured at 37 °C, pH 7.4 and 9.4 T. (Stored at 4 °C)

AGENT	**r_1 ($mM^{-1}s^{-1}$)**	**r_2 ($mM^{-1}s^{-1}$)**	**r_1 ($mM^{-1}s^{-1}$)**	**r_2 ($mM^{-1}s^{-1}$)**
	1.4 T	**1.4 T**	**9.4 T**	**9.4 T**
LipoA	1.67×10^3	2.28×10^3	1.7×10^3	1.3×10^4
LipoB	2.6×10^4	4.0×10^4	2.8×10^4	1.9×10^5
LipoC	7.8×10^3	2.3×10^4	1.3×10^4	7.3×10^4

Table S3. r_1 and r_2 proton relaxivity values based on iron liposome (per-particle) concentration[a]

[a]Values are reported at 9.4 T (37 °C) and 1.4 T (34 °C), pH 6.8-7.2. The total lipid concentration was converted into liposome concentration by approximation of the number of lipid molecules in a liposome of 100 nm size. A plot of R_1 versus liposome concentration gave the per particle relaxivity.

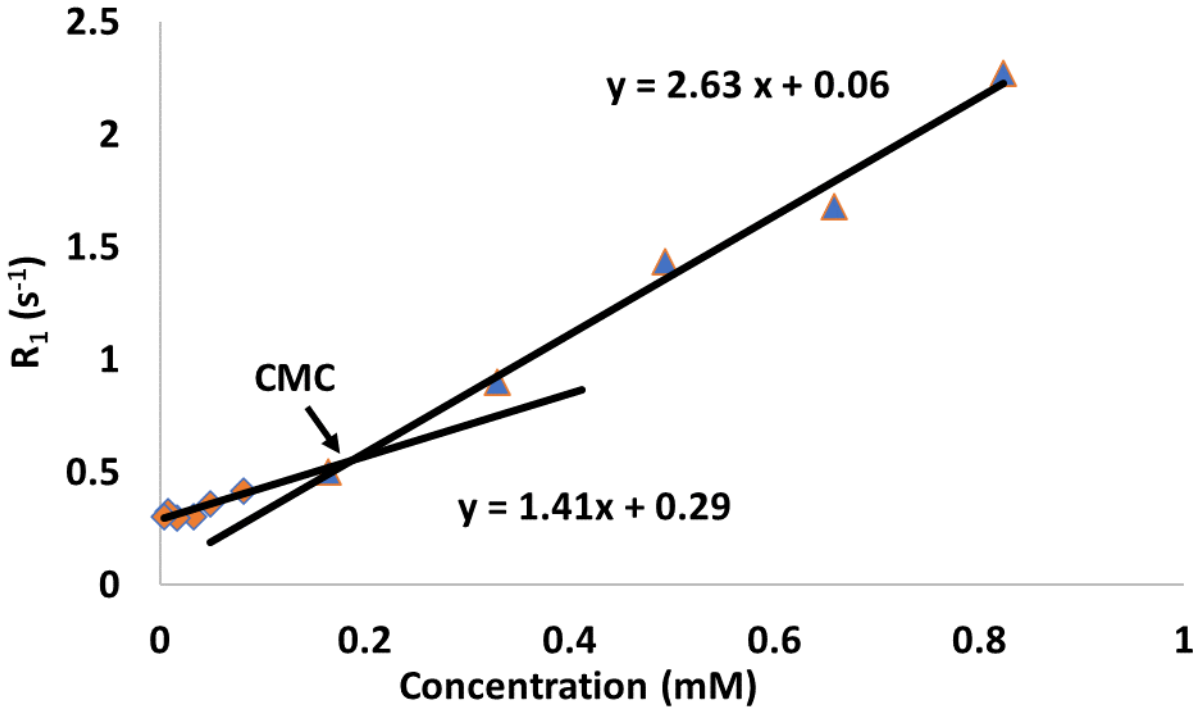

Figure S12. CMC determination for $[Fe(TOAL)]^{2+}$ micelles at 1.4T and 34 °C.

A break at 0.19 mM concentration for $[Fe(TOAL)]^{2+}$ micelle was observed indicating the presence of CMC.

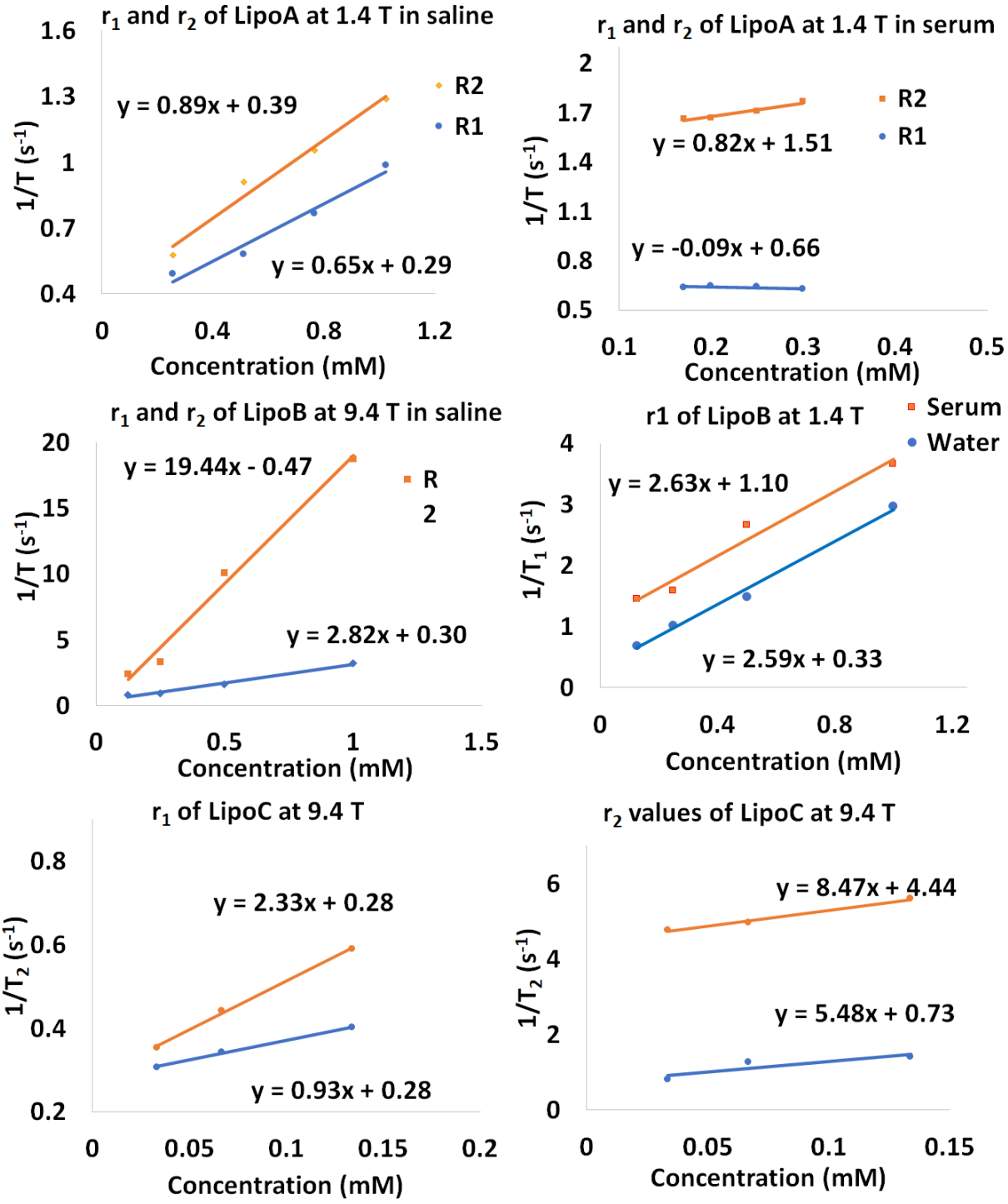

Figure S13. Sample r_1 and r_2 proton relaxivities of LipoA, LipoB and LipoC liposomes in aqueous/serum solutions at 1.4 T (34 °C) / 9.4 T (37 °C) as a function of liposome iron concentration. The relaxivities from the slopes are reported in Table 1. For the lower four graphs, orange is for experiments in serum and blue is in saline.

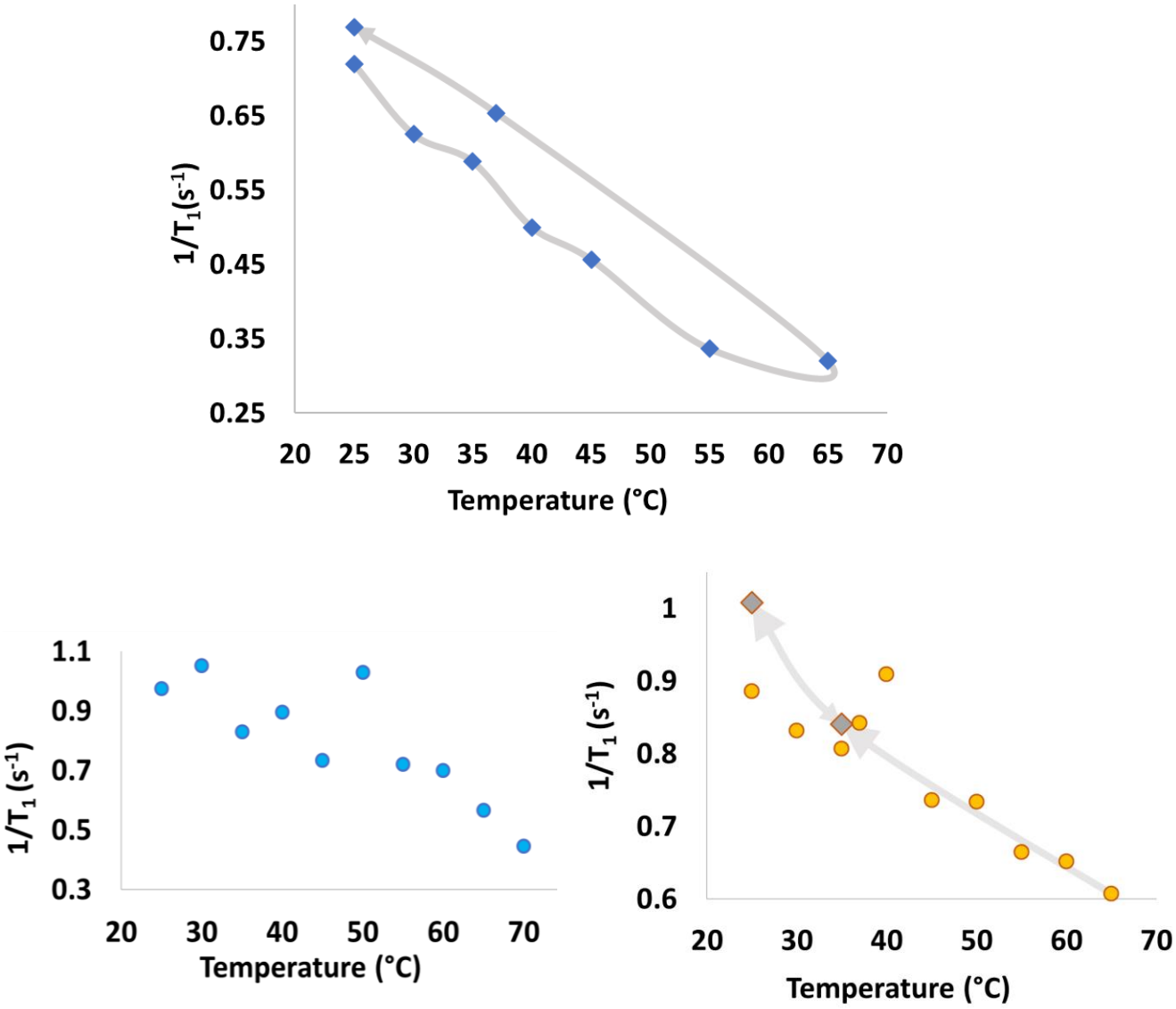

Figure S14. $1/T_1$ dependence on temperature for LipoA (top), LipoB (left) and LipoC (right) sample; Temperature was increased at 5°C steps from 25 °C to 65-70 °C and then decreased to 25 °C. Each incubation was for 7 minutes. Lines are drawn to connect the sequential data points during cooling.

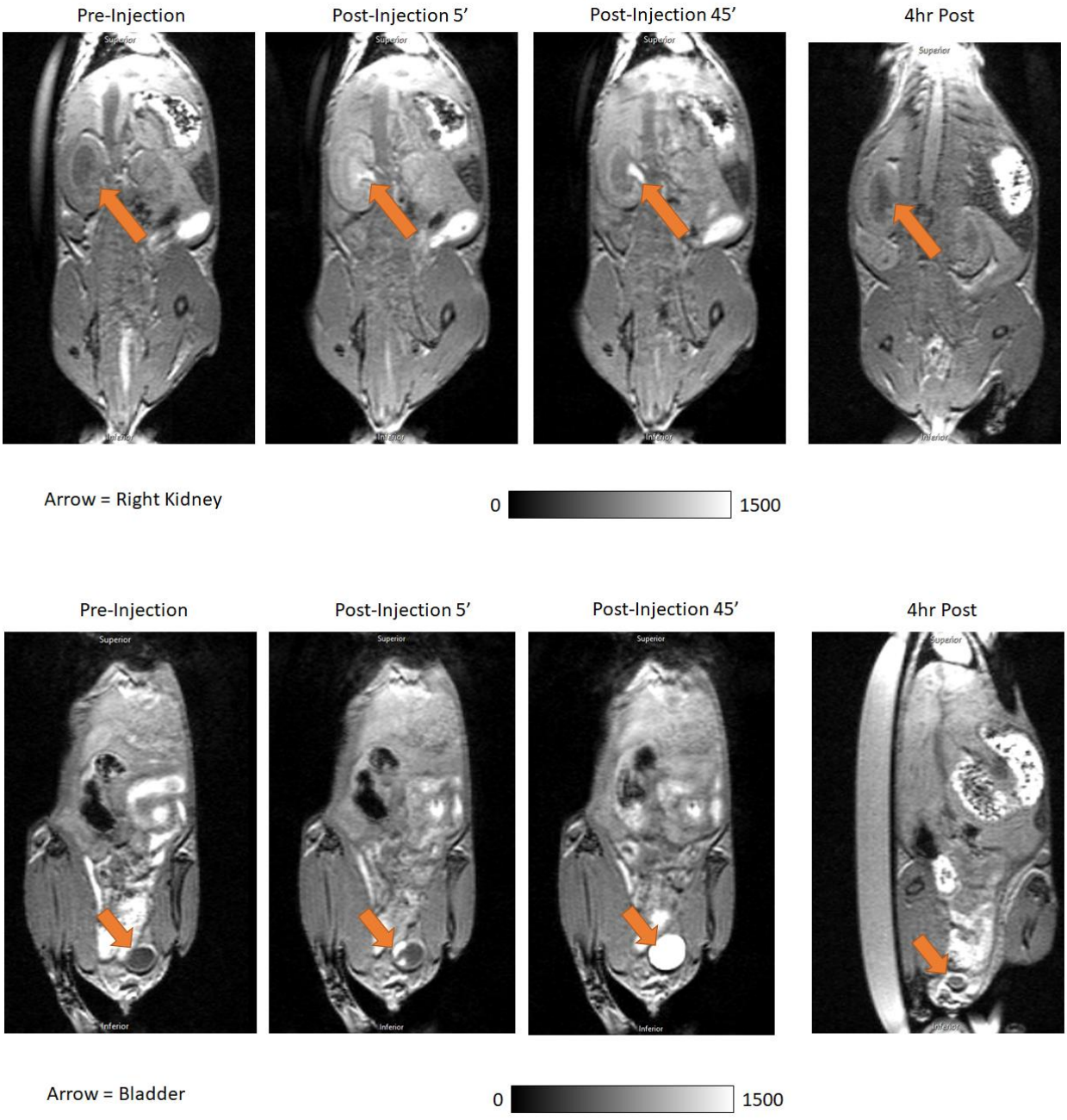

Figure S15. Biodistribution and clearance of LipoA in a healthy BALB/c mouse; Dose was 50 µmol/kg iron. Orange arrow shows Kidney (top) and bladder (bottom)

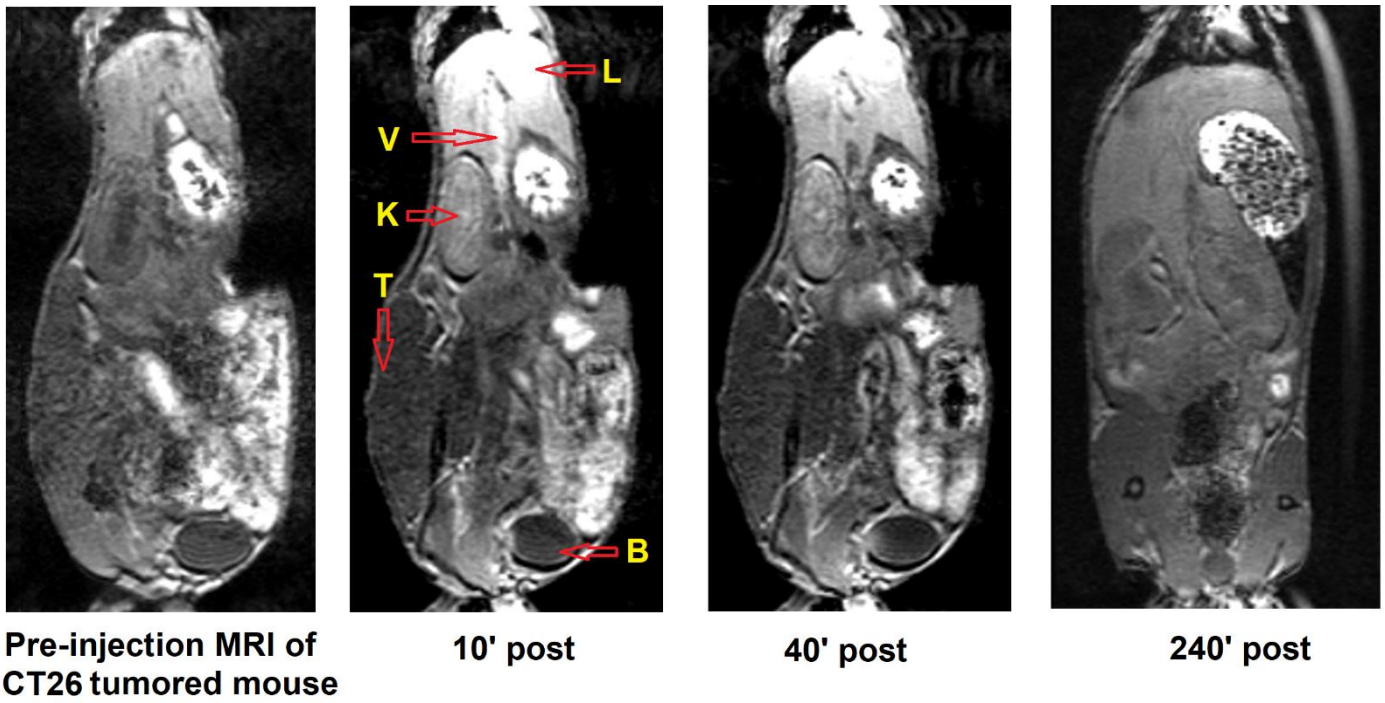

Figure S16. Biodistribution and clearance of LipoB in a CT26 tumored BALB/c mice; Dose was 50 µmol iron per kg. Distribution to Tumor (T), Liver (L), Vena cava (V), Kidney (K) and Bladder (B) are highlighted in 10' post LipoB injection MRI.

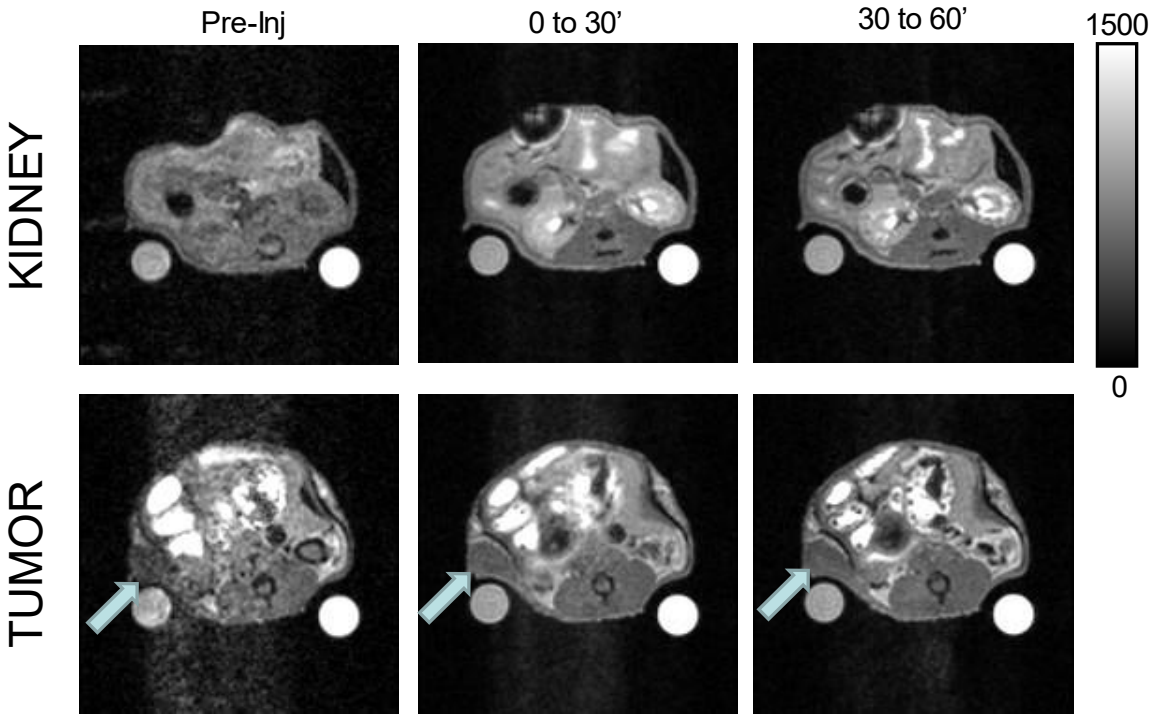

Figure S17. Biodistribution and clearance of LipoC in a CT26 tumored BALB/c mice; Dose- 100 µmol Fe(III) per kg of mouse body weight.

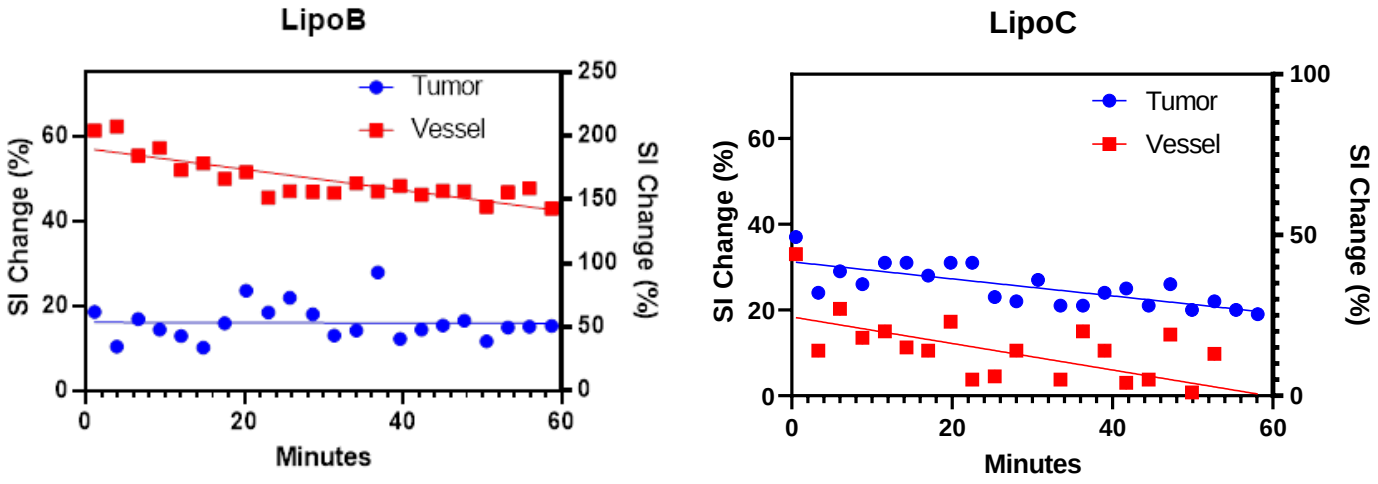

Figure S18. Change in T_1-weighted signal intensity for LipoB (50 µmol [Fe] /kg) and LipoC (125 µmol [Fe] /kg) in CT26 murine tumor over time compared to signal in blood vessel.

	LipoA	**LipoB**	**LipoC**
Fe(III) CA Dose (µmol/Kg)	**55.0**	**50.0**	**100**
1st order 'k' (min^{-1})	**6.7×10^{-2}**	**9.9×10^{-3}**	**3.4×10^{-2}**
$t_{1/2}$ (min)	**10.3**	**70.0**	**20.3**
Ratio of V_d 2-3 min after injection (ml)	**3.2**	**1.2**	**11**

Table S4. Dose, first order elimination rate constants, half-lives and volume of distribution (V_d) ratio at 2-3 min after LipoA, LipoB and LipoC injections. $V_d = dose/C_p$; $V_d \propto \frac{dose}{\Delta Signal/R_{1,obs}}$. R_{1obs} of LipoA, LipoB and LipoC in serum were 0.60, 1.8 and 1.7 respectively for calculation at their administered concentration.

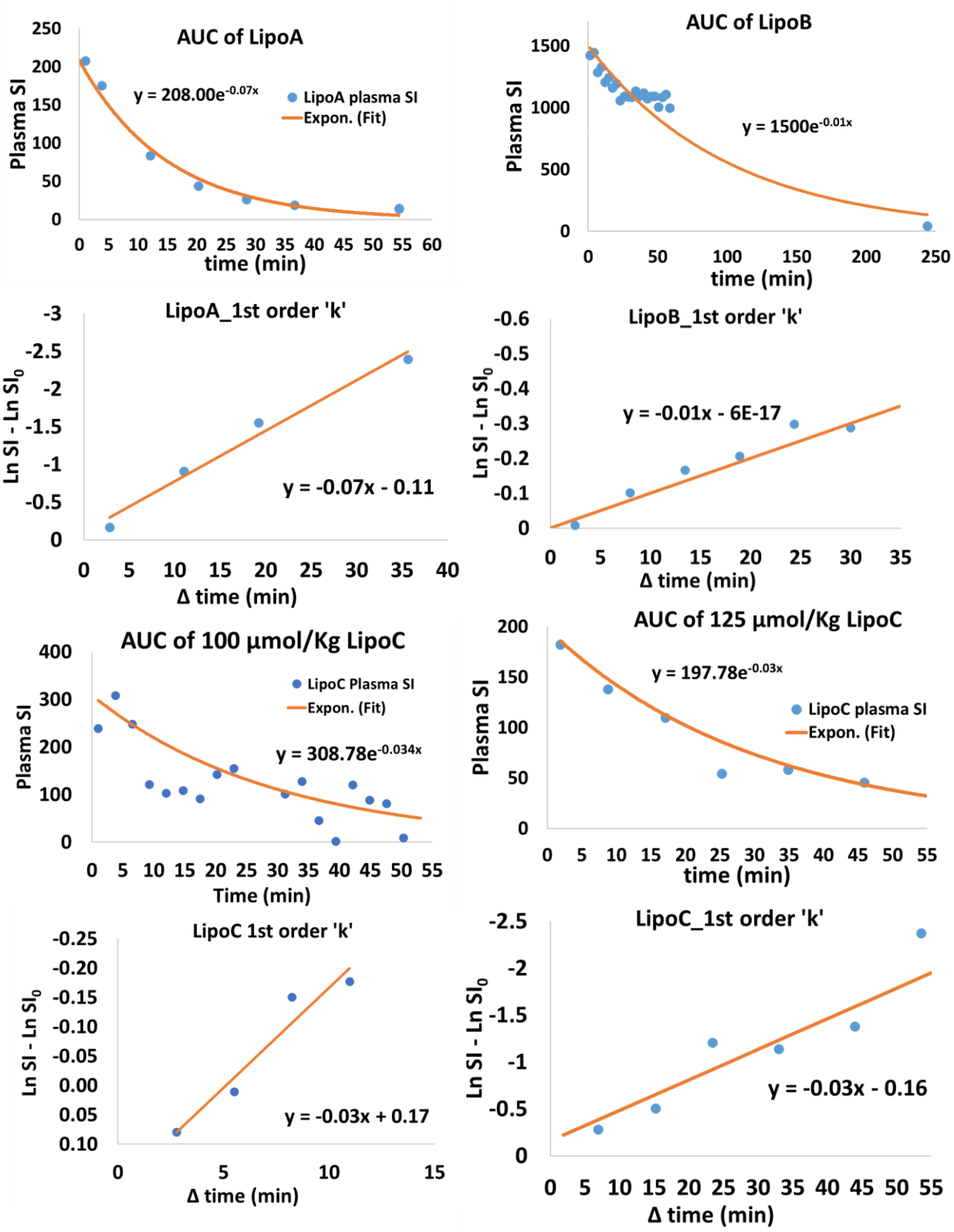

Figure S19. AUC graph and elimination rate constants of LipoA, LipoB and LipoC in Vena Cava

Temperature (°C):	25.0	**Duration Used (s):**	70
Count Rate (kcps):	207.5	**Measurement Position (mm):**	3.00
Cell Description:	Disposable low volume cuvette (50µL)	**Attenuator:**	10

			Size (d.nm):	**% Intensity:**	**St Dev (d.nm):**
Z-Average (d.nm):	106.4	**Peak 1:**	125.2	100.0	46.27
PdI:	0.148	**Peak 2:**	0.000	0.0	0.000
Intercept:	0.906	**Peak 3:**	0.000	0.0	0.000
Result quality :	Good				

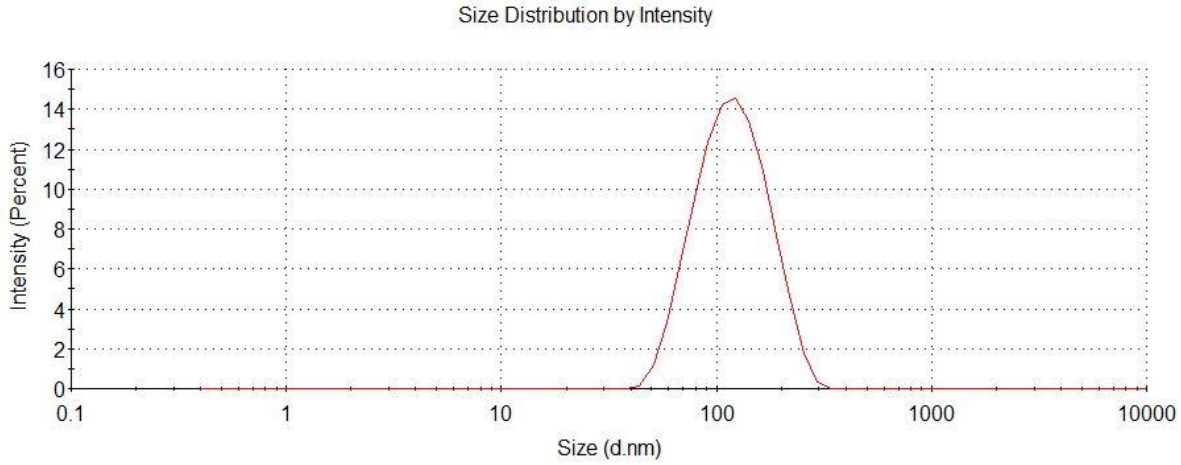

Figure S20a. DLS size measurement of dialyzed LipoA liposomes

Temperature (°C):	25.0			**Duration Used (s):**	60
Count Rate (kcps):	309.6			**Measurement Position (mm):**	3.00
Cell Description:	Disposable low volume cuvette (50µL)			**Attenuator:**	9

			Size (d.nm):	**% Intensity:**	**St Dev (d.nm):**
Z-Average (d.nm):	107.3	**Peak 1:**	125.0	100.0	58.28
PdI:	0.252	**Peak 2:**	0.000	0.0	0.000
Intercept:	0.896	**Peak 3:**	0.000	0.0	0.000
Result quality :	Good				

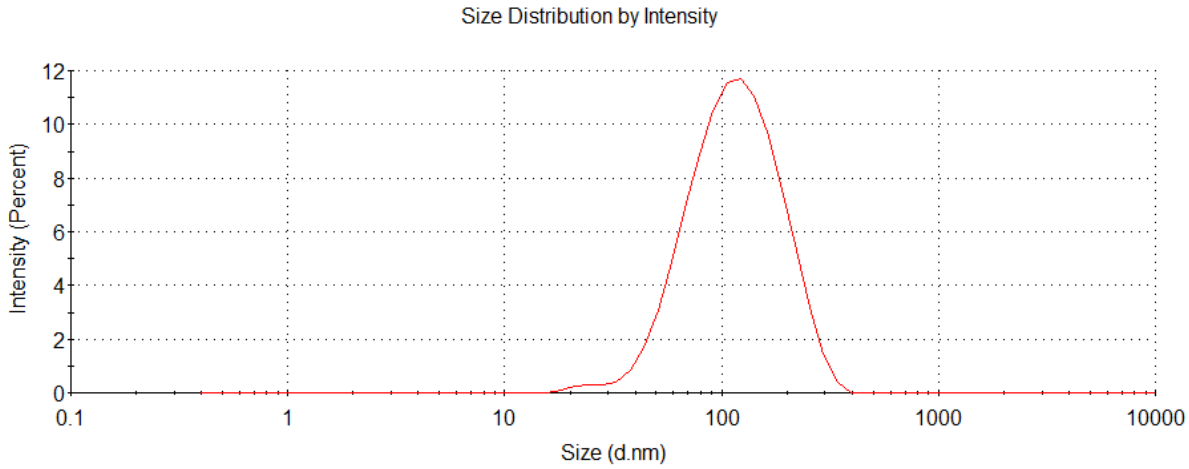

Figure S20b. DLS size measurement of dialyzed LipoB liposomes

Temperature (°C):	25.0		**Duration Used (s):**	70
Count Rate (kcps):	184.9		**Measurement Position (mm):**	3.00
Cell Description:	Disposable low volume cuvette (50µL)		**Attenuator:**	9

			Size (d.nm):	**% Intensity:**	**St Dev (d.nm):**
Z-Average (d.nm):	97.83	**Peak 1:**	111.7	100.0	39.99
PdI:	0.156	**Peak 2:**	0.000	0.0	0.000
Intercept:	0.901	**Peak 3:**	0.000	0.0	0.000
Result quality :	Good				

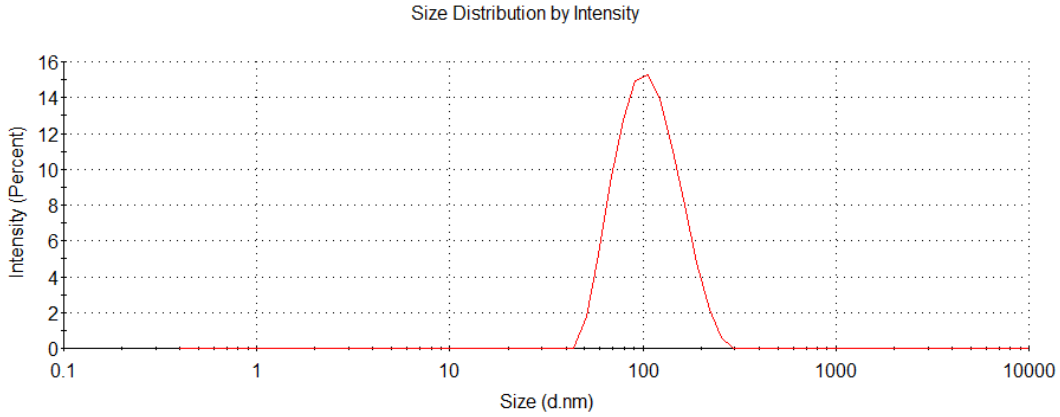

Figure S20c. DLS size measurement of dialyzed LipoC liposomes

Sample Name:	FeToal_micelle 1		
SOP Name:	new mmsop.sop		
File Name:	2023_03_28_Saiful.dts	**Dispersant Name:**	Water
Record Number:	127	**Dispersant RI:**	1.330
Material RI:	1.59	**Viscosity (cP):**	0.8872
Material Absorbtion:	0.010	**Measurement Date and Time:**	Tuesday, April 4, 2023 5:29:50 P

Temperature (°C):	25.0			**Duration Used (s):**	80
Count Rate (kcps):	131.4			**Measurement Position (mm):**	4.65
Cell Description:	Glass cuvette with square aperture			**Attenuator:**	10

			Size (d.nm):	**% Volume:**	**St Dev (d.n...**
Z-Average (d.nm):	93.10	**Peak 1:**	102.7	4.7	33.66
PdI:	0.335	**Peak 2:**	17.01	94.6	2.443
Intercept:	0.800	**Peak 3:**	2418	0.6	336.3

Result quality : **Refer to quality report**

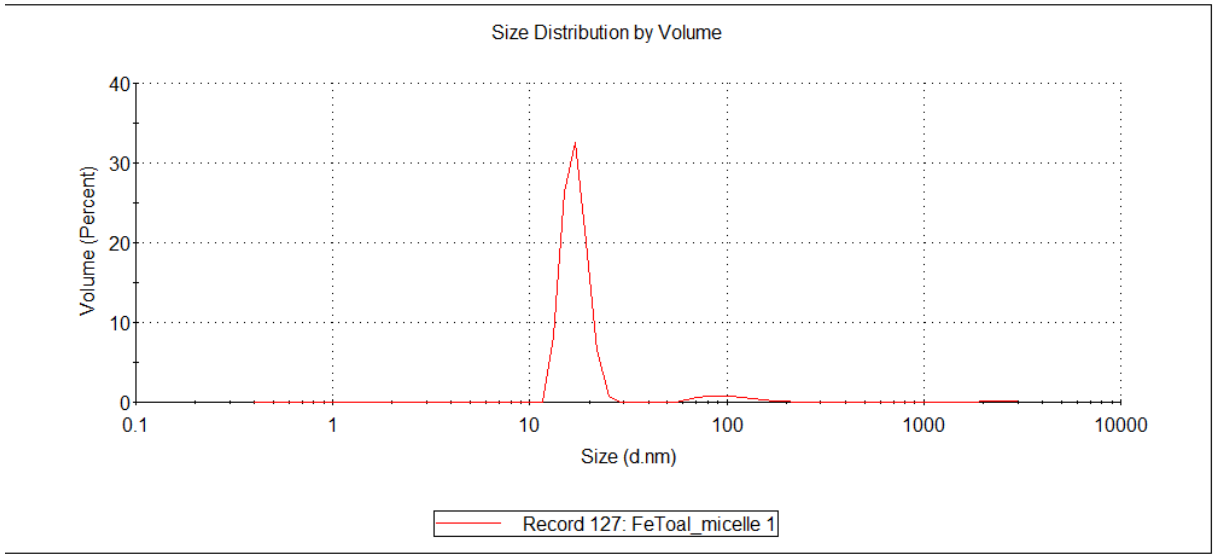

Figure 20d. DLS size measurement of FeTOAL micelle

$$Total\ number\ of\ lipid\ per\ liposome, N_{tot} = \frac{4 \times \pi \times (r-h)^2 + 4 \times \pi \times (r)^2}{Lipid\ head\ group\ average\ surface\ area}$$

$$Number\ of\ Liposomes, N_{Lipo} = \frac{Liposome\ volume\ (L) \times Liposome\ concentration\ (M) \times Number\ of\ Avogadro}{Total\ number\ of\ lipid\ per\ liposome, N_{tot}}$$

$$Permeability, P_w = \frac{1000 \times d^{inner} \times r_1^{overall} \times r_1^{inner} \times [CA]^{inner}}{6(r_1^{inner} - r_1^{overall})} \quad (1)$$

$$Water\ residence\ time, \tau = \frac{d^{inner}}{6 \times P_w} \quad (2)$$

$$r_{1,\ in} = \frac{f_{in}}{v_{in}} \times r_{1,\ CA} \quad (3)$$

$$r_{1,\ out} = (1 - f_{in}) \times r_{1,\ CA} \quad (4)$$

$$r_1 = r_{1,\ out} + \frac{v_{in}}{\frac{1}{r_{1,\ in}} + \tau} \quad (5)$$

The water permeability of the liposomal membranes was determined following a method described by Terreno and co-workers[1] and later used in another work by Peters et al[2]. The unencapsulated Fe(NOTP) was removed by dialysis for 24 - 48 h at 4˚C . A value of 11.5×10^{-5} cm.s^{-1} was found for LipoA for the P_w. The water residence time of LipoA was found 13.8 µs at 34 °C and 1.4 T.

For LipoA, LipoB and LipoC, v_{in} = 0.0297, 0.0319 and 0.0145 were estimated from the volume and per mM concentration of [CA] in liposomes.

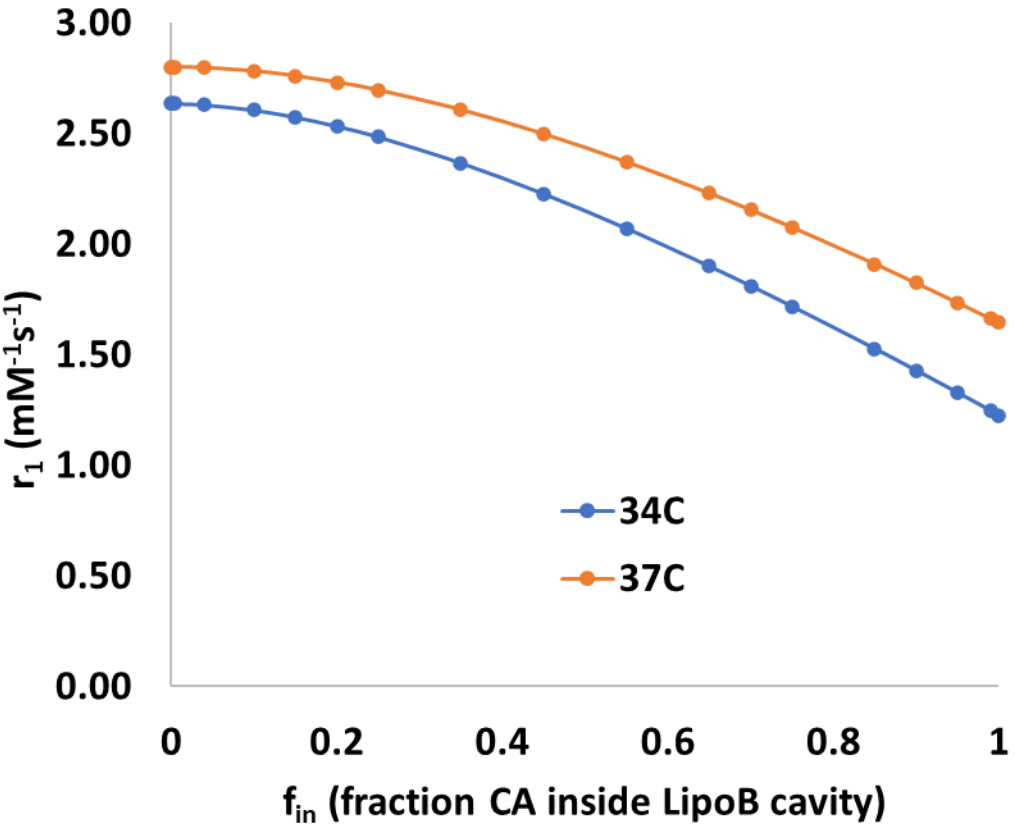

Figure 21. The relaxivity of LipoB as a function of the fraction of the contrast agent that are inside the liposomal core, as calculated with equations 3-5 at 34 °C, 1.4 T, 37 °C at 9.4 T.

References

(1) Terreno, E.; Sanino, A.; Carrera, C.; Castelli, D. D.; Giovenzana, G. B.; Lombardi, A.; Mazzon, R.; Milone, L.; Visigalli, M.; Aime, S. Determination of water permeability of paramagnetic liposomes of interest in MRI field. *J. Inorg. Biochem.* **2008**, *102*, 1112-1119.

(2) Schühle, D. T.; van Rijn, P.; Laurent, S.; Vander Elst, L.; Muller, R. N.; Stuart, M. C. A.; Schatz, J.; Peters, J. A. Liposomes with conjugates of a calix[4]arene and a Gd-DOTA derivative on the outside surface; an efficient potential contrast agent for MRI. *Chem Commun* **2010**, *46*, 4399-4401.